in women). However, these properties are not sufficient to explain the gender difference of the effect of alcohol intake on serum adiponectin concentrations. The small number of drinkers among our female subjects (15%) might cause difficulty in evaluating this result. Further study, including increasing the number female drinkers enrolled, is necessary to examine this inference.

There are potential limitations to this study. Because of its cross-sectional nature, this study did not provide a causal inference regarding the association between alcohol intake and serum adiponectin levels. However, information on the drinking habits of subjects was determined before the measurement of adiponectin concentrations; thus, an incorrect finding of an inverse association is unlikely. Data on drinking habits was based on face-to-face interviews, which leads to the possibility of misclassification of exposure (*e.g.* underreporting). However, it is also unlikely that this type of misclassification is directly dependent on adiponectin levels, which could be a nondifferential misclassification. Because our study subjects were recruited from participants in a health screening program, any generalization of these results to the normal population should be made with caution.

In conclusion, alcohol consumption was weakly associated with decreased serum adiponectin concentrations in apparently healthy Japanese subjects. Further investigations in Japanese subjects on alcohol metabolism and nutrition intake are necessary to clarify the factors that modulate this inverse effect, which differs from that seen in White subjects.

Acknowledgments

We thank Mr. Kazuo Goto, the Center for Disease Control and Prevention in Takahata, for his assistance with data collection.

Address all correspondence and requests for reprints to: Yuko Nishise, M.D., Department of Gastroenterology, Yamagata University School of Medicine, 2-2-2 Iida-Nishi, Yamagata 990-9585, Japan. E-mail: ynishise-gi@umin.ac.jp.

This study was partly funded by a Grant-in-Aid from the Global COE program of the Japan Society for the Promotion of Science.

The corresponding author had full access to all data in the study and had final responsibility for the decision to submit for publication.

Disclosure Summary: The authors have nothing to disclose.

References

1. **Chandran M, Phillips SA, Ciaraldi T, Henry RR** 2003 Adiponectin: more than just another fat cell hormone? Diabetes Care 26:2442–2450
2. **Hotta K, Funahashi T, Arita Y, Takahashi M, Matsuda M, Okamoto Y, Iwahashi H, Kuriyama H, Ouchi N, Maeda K, Nishida M, Kihara S, Sakai N, Nakajima T, Hasegawa K, Muraguchi M, Ohmoto Y, Nakamura T, Yamashita S, Hanafusa T, Matsuzawa Y** 2000 Plasma concentrations of a novel, adipose-specific protein, adiponectin, in type 2 diabetic patients. Arterioscler Thromb Vasc Biol 20:1595–1599
3. **Pischon T, Girman CJ, Hotamisligil GS, Rifai N, Hu FB, Rimm EB** 2004 Plasma adiponectin levels and risk of myocardial infarction in men. JAMA 291:1730–1737
4. **Schulze MB, Shai I, Rimm EB, Li T, Rifai N, Hu FB** 2005 Adiponectin and future coronary heart disease events among men with type 2 diabetes. Diabetes 54:534–539
5. **Daimon M, Oizumi T, Saitoh T, Kameda W, Hirata A, Yamaguchi H, Ohnuma H, Igarashi M, Tominaga M, Kato T** 2003 Decreased serum levels of adiponectin are a risk factor for the progression to type 2 diabetes in the Japanese Population: the Funagata study. Diabetes Care 26:2015–2020
6. **Suh I, Shaten BJ, Cutler JA, Kuller LH** 1992 Alcohol use and mortality from coronary heart disease: the role of high-density lipoprotein cholesterol. The Multiple Risk Factor Intervention Trial Research Group. Ann Intern Med 116:881–887
7. **Ridker PM, Vaughan DE, Stampfer MJ, Glynn RJ, Hennekens CH** 1994 Association of moderate alcohol consumption and plasma concentration of endogenous tissue-type plasminogen activator. JAMA 272:929–933
8. **Xu A, Wang Y, Keshaw H, Xu LY, Lam KS, Cooper GJ** 2003 The fat-derived hormone adiponectin alleviates alcoholic and nonalcoholic fatty liver diseases in mice. J Clin Invest 112:91–100
9. **You M, Considine RV, Leone TC, Kelly DP, Crabb DW** 2005 Role of adiponectin in the protective action of dietary saturated fat against alcoholic fatty liver in mice. Hepatology 42:568–577
10. **Ferris WF, Naran NH, Crowther NJ, Rheeder P, van der Merwe L, Chetty N** 2005 The relationship between insulin sensitivity and serum adiponectin levels in three population groups. Horm Metab Res 37:695–701
11. **Anand SS, Yusuf S, Vuksan V, Devanesen S, Teo KK, Montague PA, Kelemen L, Yi C, Lonn E, Gerstein H, Hegele RA, McQueen M** 2000 Differences in risk factors, atherosclerosis, and cardiovascular disease between ethnic groups in Canada: the Study of Health Assessment and Risk in Ethnic groups (SHARE). Lancet 356:279–284
12. **Konta T, Hao Z, Abiko H, Ishikawa M, Takahashi T, Ikeda A, Ichikawa K, Takasaki S, Kubota I** 2006 Prevalence and risk factor analysis of microalbuminuria in Japanese general population: the Takahata study. Kidney Int 70:751–756
13. **Koyano S, Emi M, Saito T, Makino N, Toriyama S, Ishii M, Kubota I, Kato T, Kawata S** 2008 Common null variant, Arg192Stop, in a G-protein coupled receptor, olfactory receptor 1B1, associated with decreased serum cholinesterase activity. Hepatology Research 38: 696–703
14. **Takeishi Y, Toriyama S, Takabatake N, Shibata Y, Konta T, Emi M, Kato T, Kawata S, Kubota I** 2007 Linkage disequilibrium analyses of natriuretic peptide precursor B locus reveal risk haplotype conferring high plasma BNP levels. Biochem Biophys Res Commun 362:480–484
15. **Kawado M, Suzuki S, Hashimoto S, Tokudome S, Yoshimura T, Tamakoshi A** 2005 Smoking and drinking habits five years after baseline in the JACC study. J Epidemiol 15(Suppl 1):S56–S66
16. **Pischon T, Girman CJ, Rifai N, Hotamisligil GS, Rimm EB** 2005 Association between dietary factors and plasma adiponectin concentrations in men. Am J Clin Nutr 81:780–786
17. **Kawamoto R, Kohara K, Tabara Y, Miki T, Ohtsuka N, Kusunoki T, Abe M** 2009 Alcohol consumption is associated with decreased insulin resistance independent of body mass index in Japanese community-dwelling men. Tohoku J Exp Med 218:331–337
18. **Nakashima R, Kamei N, Yamane K, Nakanishi S, Nakashima A, Kohno N** 2006 Decreased total and high molecular weight adiponectin are independent risk factors for the development of type 2

diabetes in Japanese-Americans. J Clin Endocrinol Metab 91:3873–3877
19. **Beulens JW, van Loon LJ, Kok FJ, Pelsers M, Bobbert T, Spranger J, Helander A, Hendriks HF** 2007 The effect of moderate alcohol consumption on adiponectin oligomers and muscle oxidative capacity: a human intervention study. Diabetologia 50:1388–1392
20. **Snijder MB, Heine RJ, Seidell JC, Bouter LM, Stehouwer CD, Nijpels G, Funahashi T, Matsuzawa Y, Shimomura I, Dekker JM** 2006 Associations of adiponectin levels with incident impaired glucose metabolism and type 2 diabetes in older men and women: the Hoorn Study. Diabetes Care 29:2498–2503
21. **López-Bermejo A, Botas P, Funahashi T, Delgado E, Kihara S, Ricart W, Fernández-Real JM** 2004 Adiponectin, hepatocellular dysfunction and insulin sensitivity. Clin Endocrinol (Oxf) 60:256–263
22. **Cnop M, Havel PJ, Utzschneider KM, Carr DB, Sinha MK, Boyko EJ, Retzlaff BM, Knopp RH, Brunzell JD, Kahn SE** 2003 Relationship of adiponectin to body fat distribution, insulin sensitivity and plasma lipoproteins: evidence for independent roles of age and sex. Diabetologia 46:459–469
23. **Lieber CS** 1995 Medical disorders of alcoholism. N Engl J Med 333:1058–1065
24. **Dohmen K, Baraona E, Ishibashi H, Pozzato G, Moretti M, Matsunaga C, Fujimoto K, Lieber CS** 1996 Ethnic differences in gastric sigma-alcohol dehydrogenase activity and ethanol first-pass metabolism. Alcohol Clin Exp Res 20:1569–1576
25. **Baraona E, Yokoyama A, Ishii H, Hernández-Muñoz R, Takagi T, Tsuchiya M, Lieber CS** 1991 Lack of alcohol dehydrogenase isoenzyme activities in the stomach of Japanese subjects. Life Sci 49:1929–1934
26. **Goedde HW, Agarwal DP, Fritze G, Meier-Tackmann D, Singh S, Beckmann G, Bhatia K, Chen LZ, Fang B, Lisker R, Paik YK, Rothhammer F, Saha N, Segal B, Srivastava LM, Czeizel A** 1992 Distribution of ADH2 and ALDH2 genotypes in different populations. Hum Genet 88:344–346
27. **Bosron WF, Lumeng L, Li TK** 1988 Genetic polymorphism of enzymes of alcohol metabolism and susceptibility to alcoholic liver disease. Mol Aspects Med 10:147–158
28. **Hsiang CY, Wu SL, Cheng SE, Ho TY** 2005 Acetaldehyde-induced interleukin-1β and tumor necrosis factor-α production is inhibited by berberine through nuclear factor-κB signaling pathway in HepG2 cells. J Biomed Sci 12:791–801
29. **Wang B, Jenkins JR, Trayhurn P** 2005 Expression and secretion of inflammation-related adipokines by human adipocytes differentiated in culture: integrated response to TNF-α. Am J Physiol Endocrinol Metab 288:E731–E740
30. **Li L, Yang G, Li Q, Tang Y, Li K** 2006 High-fat- and lipid-induced insulin resistance in rats: the comparison of glucose metabolism, plasma resistin and adiponectin levels. Ann Nutr Metab 50:499–505
31. **Chen X, Sebastian BM, Nagy LE** 2007 Chronic ethanol feeding to rats decreases adiponectin secretion by subcutaneous adipocytes. Am J Physiol Endocrinol Metab 292:E621–E628
32. **Nanji AA, Jokelainen K, Tipoe GL, Rahemtulla A, Dannenberg AJ** 2001 Dietary saturated fatty acids reverse inflammatory and fibrotic changes in rat liver despite continued ethanol administration. J Pharmacol Exp Ther 299:638–644
33. **Nanji AA, Zakim D, Rahemtulla A, Daly T, Miao L, Zhao S, Khwaja S, Tahan SR, Dannenberg AJ** 1997 Dietary saturated fatty acids down-regulate cyclooxygenase-2 and tumor necrosis factor alfa and reverse fibrosis in alcohol-induced liver disease in the rat. Hepatology 26:1538–1545
34. **Iso H, Date C, Noda H, Yoshimura T, Tamakoshi A** 2005 Frequency of food intake and estimated nutrient intake among men and women: the JACC Study. J Epidemiol 15(Suppl 1):S24–S42
35. **Baraona E, Abittan CS, Dohmen K, Moretti M, Pozzato G, Chayes ZW, Schaefer C, Lieber CS** 2001 Gender differences in pharmacokinetics of alcohol. Alcohol Clin Exp Res 25:502–507

Hepatology Research 2010; 40: 432–437 doi: 10.1111/j.1872-034X.2009.00612.x

Short Communication

Expression of the RNA-binding protein Musashi1 in adult liver stem-like cells

Etsuko Hattori,[1,*] Hong-Jin Shu,[1,*] Takafumi Saito,[1] Kazuo Okumoto,[1] Hiroaki Haga,[1] Junji Yokozawa,[1] Junitsu Ito,[1] Hisayoshi Watanabe,[1] Koji Saito,[1] Hitoshi Togashi[2] and Sumio Kawata[1]

[1]*Department of Gastroenterology, Yamagata University School of Medicine, and* [2]*Health Administrative Center, Yamagata University, Yamagata, Japan*

Aim: Musashi1 is an RNA-binding protein that regulates the Notch signaling pathway in stem cells. Our previous study revealed that Musashi1 is expressed in early hepatocytes during liver development in the mouse. However, whether this unique protein is expressed with Notch signaling markers in adult liver stem-like cells remains unknown.

Methods: Established hepatic stem-like cells (HSLC), which were derived from adult Sprague–Dawley rats, were used for experiments *in vitro*. HSLC were differentiated into mature cells in terms of producing albumin when co-cultured with epidermal growth factor (EGF). The mRNA expression of *Musashi1*, *Notch* family (*Notch1* and *Notch2*), *Jagged1* and *Hes1* was examined in HSLC before and after cell differentiation using polymerase chain reaction-based techniques. Protein expression of Musashi1 was examined in the HSLC and normal mature hepatocytes by immunofluorescence staining.

Results: The mRNA expression of *Musashi1*, *Notch1*, *Jagged1* and *Hes1* was detected in the original HSLC before culturing with EGF but not in primary cultured mature hepatocytes. The mRNA expression of *Musashi1* and *Hes1* was found to be downregulated in differentiated HSLC that produce albumin. Protein expression of Musashi1 was detectable in the original HSLC but not in both differentiated HSLC and mature hepatocytes.

Conclusion: These findings demonstrate that the RNA-binding protein Musashi1 is expressed with Notch signaling markers in adult liver stem-like cells.

Key words: hepatic stem cell, Musashi1, Notch, liver, RNA-binding protein

INTRODUCTION

IT HAS BEEN demonstrated that liver cell regeneration originates from epithelial cells through two mechanisms. First, mature hepatocytes can proliferate independently by division after the loss of liver cells, as is often observed after a partial hepatectomy.[1] An alternative mechanism, in which liver stem/progenitor cells that subsequently differentiate into hepatocytes, cholangiocytes or other liver components are produced, is involved in reconstruction of the liver after severe liver damage.[2] The signal transduction in liver stem cell differentiation has not been fully investigated.

Correspondence: Dr Takafumi Saito, Department of Gastroenterology, Yamagata University School of Medicine, 2-2-2 Iida-nishi, Yamagata 990-9585, Japan. Email: tasaitoh@med.id.yamagata-u.ac.jp
*The first two authors contributed equally to this work
Received 25 February 2009; revision 2 September 2009; accepted 11 September 2009.

Musashi1, a neural RNA-binding protein was first isolated as a mammalian homolog of the *Drosophila* protein, which is required for the asymmetric division of sensory neural precursor cells.[3] It is also known that Musashi1 is a positive regulator of the Notch signaling pathway,[4,5] which is essential for the determination of cell fate,[6] thereby maintaining the self-renewing ability of stem cells. Thus, Musashi1 is closely involved in the regulation of asymmetric cell division of stem-like cells, which generates differentiated cells.

In our previous study, we have shown that Musashi1 is expressed in early hepatocytes during liver development in the mouse.[7] Whether this unique RNA-binding protein has any association with the process of liver stem cell differentiation in adults is of considerable interest. In this study, we investigated the expression of Musashi1 in adult liver stem-like cells that regulates the Notch signaling. Our results suggest a possible association of Musashi1 in liver stem-like cell differentiation.

METHODS

Liver stem cell line and culture

AN ESTABLISHED HEPATIC epithelial stem-like cell (HSLC) line derived from the healthy liver of adult male Sprague–Dawley rats[8] was used for experiments *in vitro*. This cell line has an immature liver cell phenotype with positive expression only for α-fetoprotein and negative for both albumin and cytokeratin (CK)19, and exhibits the potential to differentiate into cells of the hepatocytic lineage and serve as stem-like cells for differentiated hepatocytes.[8] The cells were maintained in Dulbecco's modified Eagle's medium supplemented with 10% fetal bovine serum at 37°C. Spheroidal aggregates of hepatocytes are known to exhibit higher functions than hepatocytes produced by monolayer culture.[9,10] In order to demonstrate the differentiation of HSLC into cells of the hepatocytic lineage *in vitro*, the cells were co-cultured for 24 h with epidermal growth factor (EGF) at a concentration of 10 ng/mL. These cells formed spheroids in culture. The expression of albumin was examined as a marker of cell differentiation in culture cells. The mRNA expression profile for both CK19 and tyrosine aminotransferase (TAT) was also examined in HSLC before and after culturing with EGF. Primary cultured, normal adult hepatocytes were used as control cells.[11]

Western blot analysis of albumin expression in HSLC

Expression of albumin was analyzed in HSLC cultured with or without EGF. The proteins were prepared by treating the cells with cell lysis buffer, followed by centrifugation. A 15-μg sample of proteins was subjected to a 10% sodium dodecylsulfate polyacrylamide ready gel (Bio-Rad Laboratories, Richmond, CA, USA). Resolved proteins were transferred electrophoretically to an Immunobilon-P membrane (Millipore, Bedford, MA, USA) at 4°C and processed for immunodetection. After blocking with 5% nonfat milk for 1 h at room temperature, the membrane was incubated with rabbit antirat albumin antibody (1:200 dilution; Cappel, Aurora, OH, USA) at 37°C for 2.5 h. The membrane was then incubated with alkaline phosphatase-labeled goat antirabbit immunoglobulin (Ig)G antibody (1:1000 dilution; KPL, Gaithersburg, MD, USA) for 1.5 h at room temperature. Detection of the immunoreaction was performed with the BCIP/NBT phosphate substrate system (KPL), according to the manufacturer's protocol.

Reverse transcription polymerase chain reaction (RT–PCR)

The mRNA expression of *CK19*, *TAT*, *Notch* family (*Notch1* and *Notch2*) and its ligand *Jagged1*, and *Hes1* in both HSLC cultured with or without EGF and in primary cultured mature hepatocytes were examined by RT–PCR according to the procedure we previously described.[7] The PCR consisted of 35 cycles at a denaturation temperature of 94°C for 30 s, an annealing temperature of 58°C for 2 min and an extension temperature of 72°C for 1 min using a Perkin-Elmer 9600 thermal cycler platform (Perkin-Elmer, Norwalk, CT, USA). The primers for PCR to detect mRNA expression were: *Musashi1*, 5′-GGC TTCGTCACTTTCATGGACCAGGCG-3′ and 5′-GGGACC TGGTAGGTGTAAC-3′ (PCR product; 542 bp); *Hes1*, 5′-CCACTGCTACCCGTAAAGTC-3′ and 5′-GGCCTGAG GCTCTCAGTTCC-3′ (228 bp); *Notch1*, 5′-GACTATGCC TGCAGCTGTGCC-3′ and 5′-GGCTGCAGGGCACGTA GG-3′ (421 bp); *Notch2*, 5′-ATGTGTGTTACCTACCA CA-3′ and 5′-CCACAGTGGTACAGGTACTT-3′ (371 bp); *Jagged1*, 5′-CATCATAGCCTGTGAGCCTTC-3′ and 5′-ATATCATCCTCTTCCACTTCC-3′ (492 bp); CK19, 5′-TT GCGCGACAAGATTCTTGG-3′ and 5′-CATCTCACTCAG GATCTTGG-3′ (361 bp); and TAT, 5′-TGAACAGCAC TACCACTGTG-3′ and 5′-AGGCATCCTCCGTCTTCT GC-3′ (380 bp). The PCR reaction for β-actin was performed as an internal control (191 bp).[7]

Quantitation of Musashi1 mRNA levels in HSLC before and after differentiation

The total cellular RNA extracted from Hep3B cells positive for *Musashi1* mRNA expression[7] was used as a standard. The methods for RNA isolation and cDNA amplification were performed as previously.[7] To quantitate *Musashi1* mRNA levels in HSLC before and after differentiation, real-time PCR was performed using a LightCycler quick system 350S (Roche Diagnostics, Tokyo, Japan) according to the manufacturer's instructions. The primers for detection of *Musashi1* mRNA in the real-time PCR were 5′-GGCTTCGTCACTTTCATGGA CCAGGCG-3′ and 5′-GGGACCTGGTAGGTGTAAC-3′. Quantitation test was performed in quadruplicate and the results were expressed as mean ± standard error (SE). Differences at $P < 0.05$ by Mann–Whitney *U*-test were considered significant.

Immunofluorescence staining for Musashi1 in HSLC

Expression of Musashi1 was analyzed by indirect immunofluorescence staining in HSLC cultured with or

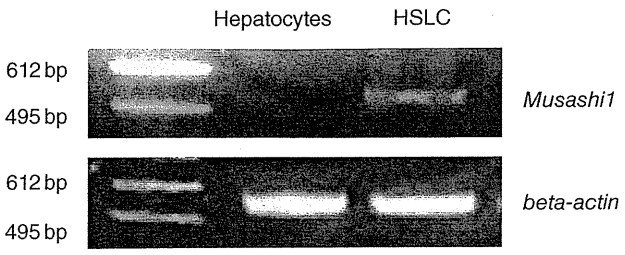

Figure 1 Reverse transcription polymerase chain reaction (RT–PCR) analysis of *Musashi1* mRNA expression in hepatic stem-like cells (HSLC) and primary cultured mature hepatocytes. The mRNA expression of *Musashi1* was detected in HSLC but not in hepatocytes. The predicted size of the PCR-amplified *Musashi1* product was 542 bp.

without EGF. A polyclonal rabbit anti-Musashi peptide antibody (Chemicon International, Temecula, CA, USA) that recognizes human and rodent Musashi1 was used as a primary antibody. Fluorescein isothiocyanate-labeled F(ab')$_2$ fragments of goat antirabbit IgG (Dako-Cytomation, Kyoto, Japan) were used as a secondary antibody. The cells were examined with the aid of a fluorescence microscope.

RESULTS

Expression of Musashi1 mRNA and Musashi1 protein in HSLC

THE MRNA EXPRESSION of *Musashi1* was detected in HSLC but not in primary cultured mature hepatocytes by RT–PCR (Fig. 1). The RT–PCR product of the *Musashi1* mRNA amplified using specific primers predicted a band of 542 bp. Protein expression of Musashi1 was detected in HSLC by immunofluorescence staining (Fig. 2), but it was not detected in primary cultured hepatocytes.

Downregulated expression of Musashi1 mRNA and Musashi1 protein in differentiated HSLC producing albumin

Hepatic stem-like cells were cultured with 10 ng/mL EGF for 24 h and harvested when they formed spheroids. Albumin expression in these cells was examined as a marker of cell differentiation from an immature to a mature state. Albumin expression was not detected in HSLC before culturing with EGF, but was detectable by western blot analysis after culturing with EGF. Quantitative analysis revealed that the level of *Musashi1* mRNA in the differentiated HSLC was significantly lower than that of original HSLC ($1.06 \pm 1.34 \times 10^{10}$ copies/mL vs $4.33 \pm 2.68 \times 10^{13}$ copies/mL, mean ± SE, $P < 0.05$) (Fig. 3). Expression of Musashi1 protein was not detected in differentiated HSLC producing albumin by immunofluorescence staining.

Changes in mRNA expression of the Notch signaling markers in HSLC differentiation

Because the expression of *Musashi1* mRNA was found to be downregulated in the cell differentiation process, the expression of the *Notch* family mRNA was investigated in HSLC before and after culturing with EGF by RT–PCR analysis. *Notch1* mRNA expression was detected in HSLC before and after culturing with EGF, but its expression was not detected in primary cultured mature hepatocytes. *Notch2* mRNA expression was found in HSLC before and after culturing with EGF as well as in primary cultured mature hepatocytes. The notch ligand *Jagged1* mRNA expression was detected in HSLC before and after culturing with EGF, but its expression was not detected in primary cultured mature hepatocytes. *Hes1* mRNA expression was detected in the original HSLC, but not in those producing albumin after culturing with EGF, and nor was it detected in primary cultured mature hepatocytes. The biliary cell marker, CK19 mRNA expression was not detected in any cells examined. The hepatocyte marker, TAT mRNA expression was not detected in the original HSLC, but its expression was detectable in those

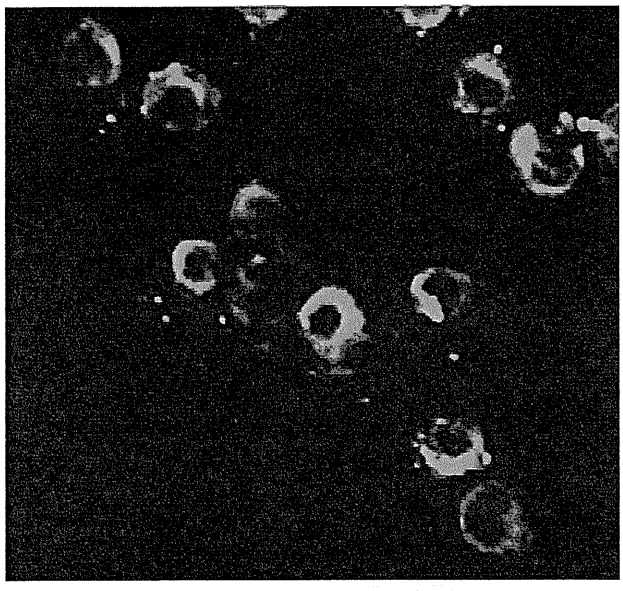

Figure 2 Immunofluorescence staining for Musashi1 protein in the cytoplasm of hepatic stem-like cells (original magnification ×400).

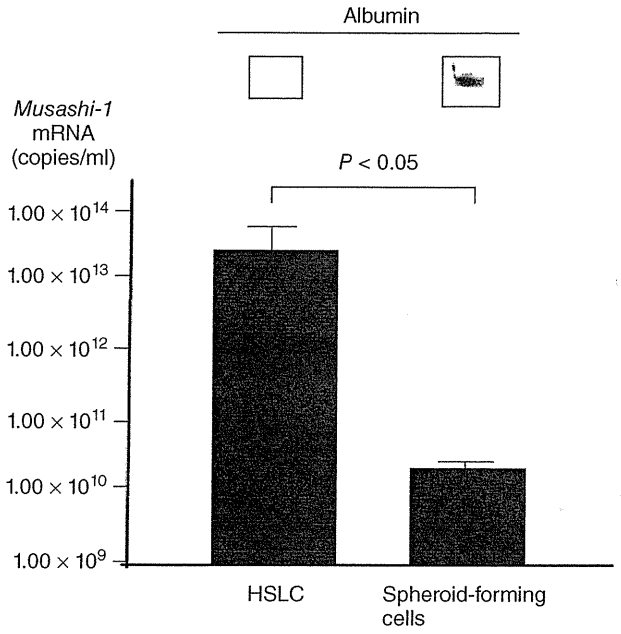

Figure 3 Western blot analysis of albumin expression in hepatic stem-like cells (HSLC). Albumin expression was not detected in the original HSLC, but was detected in spheroid-forming cells after culturing with epidermal growth factor (EGF). Real-time polymerase chain reaction analysis of *Musashi1* mRNA expression in HSLC before and after culturing with EGF. The level of *Musashi1* mRNA in the spheroid-forming differentiated cells was significantly lower than that of original HSLC. Quantitation test was performed in quadruplicate.

producing albumin after culturing with EGF as well as in primary cultured mature hepatocytes (Fig. 4).

DISCUSSION

ALTHOUGH A CLOSE association has been shown to exist between Musashi1 and Notch signaling in neural stem cell differentiation,[4] the involvement of such a mechanism in the differentiation of stem cells in digestive organs has not been fully elucidated. Recently, it was shown that Musashi1 is expressed in putative intestinal stem cells [12] and can be used as a marker of stem cells and early-lineage progenitor cells in murine intestinal tissue.

In this study, we have demonstrated that Musashi1 is expressed in putative rat liver stem-like cells at the mRNA and protein level. Interestingly, the mRNA expression of *Hes1* was downregulated along with *Musashi1* mRNA expression in the differentiated cells that produced albumin. Notch proteins were initially identified in *Drosophila* and *Caenorhabditis elegans*, but have subsequently been identified in vertebrate species.[13] It has been reported that there is an association between expression of the *Notch* family, and bile duct formation,[14] liver cell regeneration after partial hepatectomy[15] and neovascularization in the human diseased liver,[16] although no such association has been demon-

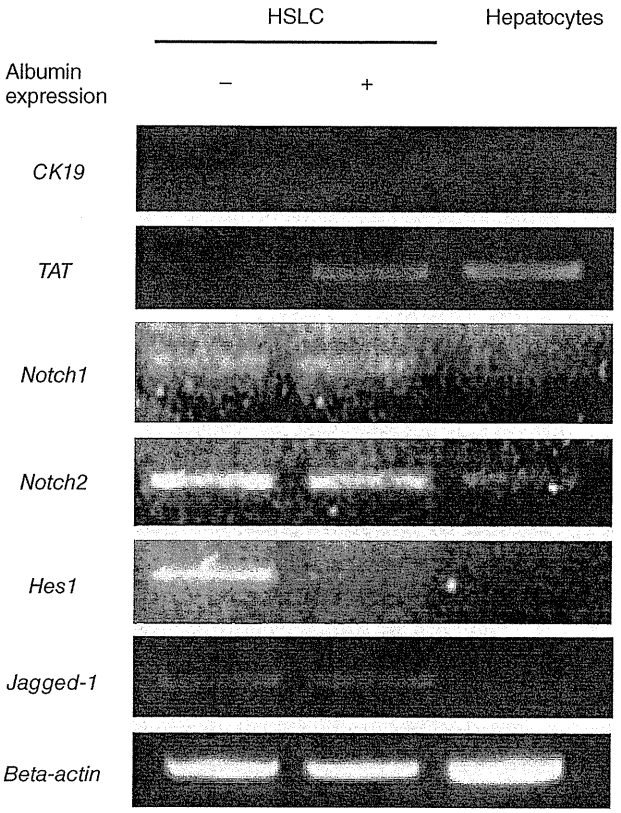

Figure 4 The mRNA expression for cytokeratin (CK)19, tyrosine aminotransferase (TAT) and *Notch* family in hepatic stem-like cells (HSLC), as revealed by reverse transcription polymerase chain reaction (RT–PCR) analysis. CK19 mRNA expression was not detected in all cells. TAT mRNA expression was not detected in the original HSLC, but it was detectable in differentiated cells producing albumin as well as in mature hepatocytes. The mRNA expression for *Notch1* and *Jagged1* was detected in HSLC, but it was not detected in mature hepatocytes. *Notch2* mRNA expression was detected in all cells. The mRNA expression of *Hes1* was detected in HSLC, but was undetectable in differentiated cells producing albumin as well as in mature hepatocytes. The predicted size of the PCR-amplified product was 361 bp for CK19, 380 bp for TAT, 421 bp for *Notch1*, 371 bp for *Notch2*, 492 bp for *Jagged-1* and 228 bp for *Hes1*.

strated in liver stem cells. Both Notch-1 and its ligand Jagged-1 have been detected in the hepatic progenitor cells, referred to as oval cells, in the liver of the 2-acetylaminofluorene 70% hepatectomy models.[17] In this study, *Notch1* and *Jagged1* mRNA expressions were detectable in HSLC , but not in mature rat hepatocytes. The absence of Notch1 expression in mature hepatocytes has also been demonstrated in humans.[17] *Hes1* mRNA expression is activated by a nuclear translocation of the Notch intracellular domain.[11] In the present study, we could show that *Hes1* mRNA expression was also detectable in HSLC at a location downstream of this signaling. The mRNA expression of *Notch1–Hes1* signaling was upregulated in Musashi1-positive HSLC and was undetectable in the differentiated cells producing albumin. To confirm the association of Musashi1 with an activation of the Notch signaling, it would be important to see if changes in Musashi1 expression level by the gene knockdown influence of liver stem-like cell differentiation. In addition, expression of Musashi1 in the liver tissue remains unknown. Further studies are needed to elucidate these issues.

The roles of Musashi1 in the development of liver morphology and function remain unknown. A report on the *Musashi1* gene disruption model revealed that homozygous newborn mice are not prone to immediate death, but frequently develop obstructive hydrocephalus with aberrant proliferation of ependymal cells.[5] As Musashi2, another member of the RNA-binding protein family,[18] is co-expressed in this model, gene compensation of *Musashi2* in the *Musashi1* disruption model might contribute to organ development, and hence improve the chances of survival. Analyses of alteration of liver-specific mRNA expression as well as liver morphology in such a model would provide information that could extend our understanding of the role of Musashi1 in the development of liver morphology and function.

In conclusion, the results of this study suggest that Musashi1 is expressed with Notch signaling markers in liver stem-like cells as well as in neural stem cells in adults. The role of Musashi1 in liver regeneration warrants further investigation.

ACKNOWLEDGEMENTS

THE AUTHORS THANK Dr Toshihiro Sugiyama for the gift of HSLC and Dr Hideyuki Okano for critical reading of the manuscript. This paper was supported by a Grant-in-Aid from the Global COE program of the Japan Society for the Promotion of Science, and in part by a grant from the Ministry of Health, Labor and Welfare of Japan.

REFERENCES

1 Bucher NL. Experimental aspects of hepatic regeneration. *N Engl J Med* 1967; 277: 686–96.
2 Thorgeirsson SS. Hepatic stem cells in liver regeneration. *FASEB J* 1996; 10: 1249–56.
3 Nakamura M, Okano H, Blendy JA, Montell C. Musashi, a neural RNA-binding protein required for Drosophila adult external sensory organ development. *Neuron* 1994; 13: 67–8.
4 Okano H, Imai T, Okabe M. Musashi: a translational regulator of cell fate. *J Cell Sci* 2002; 115: 1355–9.
5 Imai T, Tokunaga A, Yoshida T *et al.* The neural RNA-binding protein Musashi1 translationally regulates mammalian numb gene expression by interacting with its mRNA. *Mol Cell Biol* 2001; 21: 3888–900.
6 Artavanis-Tsakonas S, Rand MD, Lake RJ. Notch signaling: cell fate control and signal integration in development. *Science* 1999; 284: 770–6.
7 Shu HJ, Saito T, Watanabe H *et al.* Expression of the Musashi1 gene encoding the RNA-binding protein in human hepatoma cell lines. *Biochem Biophys Res Commun* 2002; 293: 150–4.
8 Nagai H, Terada K, Watanabe G, *et al.* Differentiation of liver epithelial (stem-like) cells into hepatocytes induced by coculture with hepatic stellate cells. *Biochem Biophys Res Commun* 2002; 293: 1420–5.
9 Matsushita T, Ijima H, Koide N, Funatsu K. High albumin production by multicellular spheroid of adult rat hepatocytes formed in the pores of polyurethane foam. *Appl Microbiol Biotechnol* 1991; 36: 324–6.
10 Tobe S, Takei Y, Kugumiya T, Kobayashi A, Kobayashi K, Akaike T. Formation mechanism and differential functionality of multiplayer hepatocyte-aggregation on artificial biomatrix. *Jpn J Artif Organs* 1992; 20: 150–5.
11 Okumoto K, Saito T, Hattori E *et al.* Differentiation of bone marrow cells into cells that express liver-specific genes *in vitro*: implication of the Notch signals in differentiation. *Biochem Biophys Res Commun* 2003; 304: 691–5.
12 Potten CS, Booth C, Tudor GL *et al.* Identification of a putative intestinal stem cell and early lineage marker; musashi-1. *Differentiation* 2003; 71: 28–41.
13 Weinmaster G. The ins and outs of Notch signaling. *Mol Cell Neurosci* 1997; 9: 91–102.
14 Kodama Y, Hijikata M, Kageyama R, Shimotohno K, Chiba T. The role of notch signaling in the development of intrahepatic bile ducts. *Gastroenterology* 2004; 127: 1775–86.
15 Kohler C, Bell AW, Bowen WC, Monga SP, Fleig W, Michalopoulos GK. Expression of Notch-1 and its ligands Jagged-1 in rat liver during liver regeneration. *Hepatology* 2004; 39: 1056–65.

16 Nijjar SS, Crosby HA, Wallace L, Hubscher SG, Strain AJ. Notch receptor expression in adult human liver: a possible role in bile duct formation and hepatic neovascularization. *Hepatology* 2001; 34: 1184–92.
17 Jensen CH, Jauho EI, Santoni-Rugiu E *et al.* Transit-amplifying ductular (oval) cells and their hepatocytic progeny are characterized by a novel and distinctive expression of delta-like protein/preadipocyte factor 1/fetal antigen 1. *Am J Pathol* 2004; **164**: 1347–1359.
18 Sakakibara S, Nakamura Y, Satoh H, Okano H. RNA-binding protein Musashi2: developmentally regulated expression in neural precursor cells and subpopulations of neurons in mammalian CNS. *J Neurosci* 2001; **21**: 8091–107.

Serum metabolomics reveals γ-glutamyl dipeptides as biomarkers for discrimination among different forms of liver disease

Tomoyoshi Soga[1,*], Masahiro Sugimoto[1], Masashi Honma[2], Masayo Mori[1], Kaori Igarashi[1], Kasumi Kashikura[1], Satsuki Ikeda[1], Akiyoshi Hirayama[1], Takehito Yamamoto[2], Haruhiko Yoshida[3], Motoyuki Otsuka[3], Shoji Tsuji[4], Yutaka Yatomi[4], Tadayuki Sakuragawa[5], Hisayoshi Watanabe[6], Kouei Nihei[7], Takafumi Saito[6], Sumio Kawata[6], Hiroshi Suzuki[2], Masaru Tomita[1], Makoto Suematsu[5]

[1]*Institute for Advanced Biosciences, Keio University, Tsuruoka 997-0052, Japan;* [2]*Department of Pharmacy, The University of Tokyo Hospital, Hongo, Bunkyo-ku, Tokyo 113-8655, Japan;* [3]*Department of Gastroenterology, Faculty of Medicine, The University of Tokyo, Hongo, Bunkyo-ku, Tokyo 113-8655, Japan;* [4]*Department of Neurology, Division of Neuroscience, Graduate School of Medicine, The University of Tokyo, Hongo, Bunkyo-ku, Tokyo 113-8655, Japan;* [5]*Department of Biochemistry, JST ERATO Suematsu Gas Biology Project, School of Medicine, Keio University, Shinanomachi, Shinjuku-ku, Tokyo 160-8582, Japan;* [6]*Department of Gastroenterology, Yamagata University School of Medicine, Yamagata 990-9585, Japan;* [7]*Department of Surgery, Shonai Hospital, 4-20 Izumi-cho, Tsuruoka 997-8515, Japan*

Background & Aims: We applied a metabolome profiling approach to serum samples obtained from patients with different liver diseases, to discover noninvasive and reliable biomarkers for rapid-screening diagnosis of liver diseases.

Methods: Using capillary electrophoresis and liquid chromatography mass spectrometry, we analyzed low molecular weight metabolites in a total of 248 serum samples obtained from patients with nine types of liver disease and healthy controls.

Results: We found that γ-glutamyl dipeptides, which were biosynthesized through a reaction with γ-glutamylcysteine synthetase, were indicative of the production of reduced glutathione, and that measurement of their levels could distinguish among different liver diseases. Multiple logistic regression models facilitated the discrimination between specific and other liver diseases and yielded high areas under receiver-operating characteristic curves. The area under the curve values in training and independent validation data were 0.952 and 0.967 in healthy controls, 0.817 and 0.849 in drug-induced liver injury, 0.754 and 0.763 in asymptomatic hepatitis B virus infection, 0.820 and 0.762 in chronic hepatitis B, 0.972 and 0.895 in hepatitis C with persistently normal alanine transaminase, 0.917 and 0.707 in chronic hepatitis C, 0.803 and 0.993 in cirrhosis type C, and 0.762 and 0.803 in hepatocellular carcinoma, respectively. Several γ-glutamyl dipeptides also manifested potential for differentiating between nonalcoholic steatohepatitis and simple steatosis.

Conclusions: γ-Glutamyl dipeptides are novel biomarkers for liver diseases, and varying levels of individual or groups of these peptides have the power to discriminate among different forms of hepatic disease.

Introduction

Acute or chronic viral hepatitis affects populations around the world, and the disease often progresses from chronic hepatitis and cirrhosis to hepatocellular carcinoma (HCC) [1]. Accurate diagnosis at earlier stages is necessary for improved therapeutic outcome. However, the diagnostic procedures are laborious and not risk-free. Patients with suspected liver damage are initially subjected to liver function tests that include the assessment of aspartate transaminase (AST), alanine transaminase (ALT), and γ-glutamyl transpeptidase (γ-GTP) serum levels. If these levels are abnormal, patients are then subjected to diagnostic imaging, such as ultrasound and computed tomography (CT), and assays to determine the presence of antibodies against hepatitis virus. Finally, a liver biopsy may be recommended to evaluate the severity of inflammation or fibrosis and to confirm the indications for antiviral therapy.

Recently, nonalcoholic fatty liver disease (NAFLD) has become the most common liver disease in western countries. It

ELSEVIER

Journal of Hepatology **2011** vol. 55 | 896–905

encompasses a wide spectrum of conditions associated with over-accumulation of fat in the liver, ranging from simple steatosis (SS) to nonalcoholic steatohepatitis (NASH), and cirrhosis [2]. Although SS typically follows a benign non-progressive clinical course, NASH may eventually develop into cirrhosis and HCC. To date, a liver biopsy remains the gold standard for the diagnosis of NASH [3]. However, since the biopsy procedures carry the risk of mortality [4,5], the noninvasive identification of biomarkers, that can provide reliable differential diagnoses for the characterization of liver diseases, is desirable.

Metabolomics, which can be defined as measurement of the levels of all cellular metabolites, has emerged as a powerful new tool for discovering new low molecular weight biomarkers. Its utility has been demonstrated by the identification of new biomarkers for prostate cancer [6], Parkinson's disease [7], type 2 diabetes mellitus [8], acute myocardial ischemia [9], and pre-eclampsia [10].

Recently, we developed new metabolomic profiling approaches based on capillary electrophoresis mass spectrometry [11] and capillary electrophoresis–time-of-flight mass spectrometry (CE–TOFMS) [12–14]. The efficacy of CE–TOFMS was demonstrated by the discovery of ophthalmate (γ-glutamyl-2-aminobutyrylglycine) as a biomarker; in mice, reduced glutathione (GSH) depletion produced acetaminophen-induced hepatotoxicity [12,14]. In this study, to discover new noninvasive biomarkers for human liver diseases, we comprehensively analyzed the serum metabolites in a total of 248 samples from patients with nine types of liver disease or gastric cancer (GC) and from normal individuals using our metabolomic approaches, and found increased levels of γ-glutamyl dipeptides in the majority of the liver diseases. Moreover, we found that γ-glutamyl dipeptides were synthesized via the ligation of glutamate with various amino acids and amines by the γ-glutamylcysteine synthetase (GCS), an enzyme that is feedback-inhibited by GSH, and that the levels of γ-glutamyl dipeptides were indicative of the amount of GSH production. The concentrations of serum γ-glutamyl dipeptides varied with the stage and type of liver disease and can, therefore, act as new biomarkers for liver diseases. Here, we report that a highly specific set of γ-glutamyl dipeptides, alone or in combination with transaminases and methionine sulfoxide, can effectively distinguish specific liver diseases from other hepatic injuries and healthy control samples.

Materials and methods

Serum samples

A total of 248 serum samples were obtained from three institutes, Yamagata University Hospital (YUH; Yamagata, Japan), University of Tokyo Hospital (UTH; Tokyo, Japan) and Shonai Hospital (SH; Tsuruoka, Japan). The 162 YUH cases comprised 53 healthy controls (C) and patients with drug-induced liver injury (DI; $n = 10$), asymptomatic hepatitis B virus infection (AHB; $n = 9$), chronic hepatitis B (CHB; $n = 7$), hepatitis C with persistently normal alanine transaminase (CNALT; $n = 10$), chronic hepatitis C (CHC; $n = 24$), cirrhosis type C (CIR; $n = 10$), HCC ($n = 19$), SS ($n = 9$) and NASH ($n = 11$). The 75 UTH cases comprised four controls and patients with DI ($n = 17$), AHB ($n = 7$), CHB ($n = 7$), CNALT ($n = 8$), CHC ($n = 11$), CIR ($n = 8$) and HCC ($n = 13$). The 11 SH cases were all GC patients. Written informed consent was obtained from all the participants and the study protocol conformed to the ethical guidelines of the 1975 Declaration of Helsinki as reflected in a priori approval by the appropriate institutional review boards of YUH, UTH, and SH. The study subjects were patients with viral liver diseases, drug-induced hepatotoxicity or NAFLD who were referred to the Department of Gastroenterology and Hepatology at YUH, UTH, or SH.

Clinical diagnosis

All the healthy controls had normal liver function and no viral hepatitis infection, and none were alcoholics. The AHB and CNALT patients were confirmed to have normal liver function and to be positive for hepatitis B surface (HBs) antigen and hepatitis B virus (HBV) DNA, or for anti-hepatitis C virus (HCV) antibodies and HCV RNA, respectively. DI was diagnosed based on abnormal values on biochemical tests, absence of other hepatic diseases, and a history of treatment with drugs suspected of being probable causes of DI. The suspected medications were different, and the biochemical test results in each patient normalized after their withdrawal.

CHC and CIR were diagnosed on the basis of physical examination, biochemical tests, ultrasonography, and CT findings. Some patients with chronic hepatitis provided informed consent for a liver biopsy, and the procedure was performed to confirm the accuracy of the diagnosis. The diagnosis of CHB and CHC was based on increased ALT levels (above the upper limit of the normal range) in at least two blood samples assayed over a 6-month period, and the presence of detectable HBs antigen and HBV DNA or detectable anti-HCV antibodies and HCV RNA, respectively. HCV infection was causative in all cirrhosis patients, and they manifested symptoms of portal hypertension, such as splenomegaly, esophageal varices, encephalopathy, or ascites.

The diagnosis of HCC was based on ultrasonography, CT, and MRI findings that revealed features typical of HCC. HCV was causative in all cases, and the α-fetoprotein (AFP) and protein induced by vitamin K antagonist (PIVKA)-II levels were assayed in all HCC patients.

All of the SS and NASH patients underwent liver biopsy. The tissue samples were stained with hematoxylin–eosin, reticulin, and Masson trichrome; and examined by the same experienced pathologist who was blinded to the clinical data. The histological criterion for the diagnosis of NAFLD was the presence of fatty changes in hepatocytes. When hepatocytes exhibited macrovesicular steatosis, the differential diagnosis was SS or NASH. The criteria for a diagnosis of steatohepatitis were the presence of lobular inflammation and either ballooning cells or perisinusoidal/pericellular fibrosis, in addition to steatosis in the liver specimen. No patient with autoimmune hepatitis, primary biliary cirrhosis, sclerosing cholangitis, hemochromatosis, α1-antitrypsin deficiency, Wilson's disease, or alcoholic liver injury was included. All patients with GC were diagnosed by pathologic studies of biopsy tissues.

Analytical and statistical technologies for biomarker discovery

Using a total of 237 samples from YUH (training cohort, $n = 162$) and UTH (validation cohort, $n = 75$) (Table 1), we performed CE–TOFMS for a comprehensive analysis of the metabolite changes to discover new biomarkers in the diagnosis of human liver diseases. To facilitate peak identification and quantification, we analyzed 162 metabolic standards listed in the KEGG LIGAND database [15] before analyzing the samples. Global mass scanning over a 50–1000 m/z range was applied in the CE–TOFMS mode [12]. To focus on γ-glutamyl peptides, we employed a highly sensitive method using liquid chromatography electrospray tandem mass spectrometry (LC–MS/MS) with multiple reactions monitoring for analyses of the patient serum samples. The Kruskal–Wallis test and Dunn's post-test were used to assess the statistical significance of differences among C, DI, AHB, CHB, CNALT, CHC, CIR, and HCC. The Mann–Whitney test was used to evaluate the statistical significance of differences between SS and NASH. The algorithm of the feature selection for the multiple logistic regression (MLR) models is described in the Supplementary data.

Results

Discovery of γ-glutamyl dipeptides in serum by metabolomic profiling

The CE–TOFMS analysis quantified the levels of 49 metabolites in the serum samples (Supplementary Tables 1 and 2) and revealed increases in many compounds in most liver diseases. We identified these compounds as γ-glutamyl dipeptides (e.g., γ-Glu-Gly, γ-Glu-Ala, γ-Glu-Ser, γ-Glu-Val, γ-Glu-Thr, γ-Glu-Taurine, γ-Glu-Leu, γ-Glu-Gln, γ-Glu-Lys, γ-Glu-Glu, γ-Glu-Met, γ-Glu-His, γ-Glu-Phe, γ-Glu-Arg, γ-Glu-Citrulline, γ-Glu-Tyr, and γ-Glu-Trp) by comparing their migration times and exact molecular

Table 1. Summary of patient information.

Clinical information		Training cohort (n = 162)	Defect no.	Validation cohort (n = 75)	Defect no.	*p* value
Age (years)						
	Median	61	0	66	0	0.47
	Interquartile range	51-73	0	55-70	0	
Sex (n)	Male	73	0	52	0	0.0007*
	Female	89	0	23	0	
AST (UL^{-1})						
	C	21.5 ± 5.40	0	25.3 ± 3.60	0	0.074
	DI	274 ± 567	0	81.2 ± 84.9	0	0.15
	AHB	25.0 ± 6.81	2	23.9 ± 6.90	0	0.71
	CHB	109 ± 164	0	150 ± 146	0	0.0059
	CNALT	24.1 ± 3.80	0	23.8 ± 6.00	0	0.72
	CHC	62.8 ± 65.3	0	110 ± 51.0	0	0.0010
	CIR	54.6 ± 27.1	0	58.0 ± 26.1	0	0.69
	HCC	71.3 ± 52.8	0	35.0 ± 24.5	0	0.0010
	SS	41.2 ± 11.5	0			
	NASH	78.6 ± 48.0	0			
ALT (UL^{-1})						
	C	17.7 ± 4.70	0	25.0 ± 8.30	0	0.062
	DI	253 ± 343	0	115 ± 132	0	0.15
	AHB	26.6 ± 18.6	2	23.1 ± 5.60	0	0.40
	CHB	117 ± 162	0	173 ± 131	0	0.0060
	CNALT	17.9 ± 4.10	0	21.5 ± 3.60	0	0.074
	CHC	79.4 ± 81.0	0	160 ± 116	0	0.0036
	CIR	40.7 ± 21.9	0	57.3 ± 42.4	0	0.69
	HCC	57.9 ± 58.8	0	25.0 ± 21.6	0	0.0026
	SS	72.2 ± 24.5	0			
	NASH	121 ± 140	0			
γ-GTP						
	C	20.7 ± 8.60	0	—	4	—
	DI	190 ± 236	0	46.2 ± 29.5	5	0.010
	AHB	31.1 ± 24.1	2	—	7	—
	CHB	52.8 ± 38.1	1	—	7	—
	CNALT	150 ± 5.70	0	—	8	—
	CHC	48.5 ± 36.4	0	—	11	—
	CIR	28.8 ± 17.9	0	49.6 ± 53.1	0	0.17
	HCC	51.2 ± 31.1	0	—	13	—
	SS	61.8 ± 43.7	0			
	NASH	98.7 ± 99.1	0			
AFP						
	CHC	6.40 ± 7.40	3	—	11	—
	CIR	35.1 ± 71.8	0	14 ± 15.6	0	0.63
	HCC	9.79×10^2 ± 1.73×10^3	0	7.04×10^3 ± 2.52×10^4	0	0.024
PIVKA-II						
	HCC	1.57×10^2 ± 1.87×10^2	0	7.78×10^3 ± 2.77×10^4	0	0.022

*Chi-square test. The others *p* values were obtained by the Mann–Whitney *U*-test.

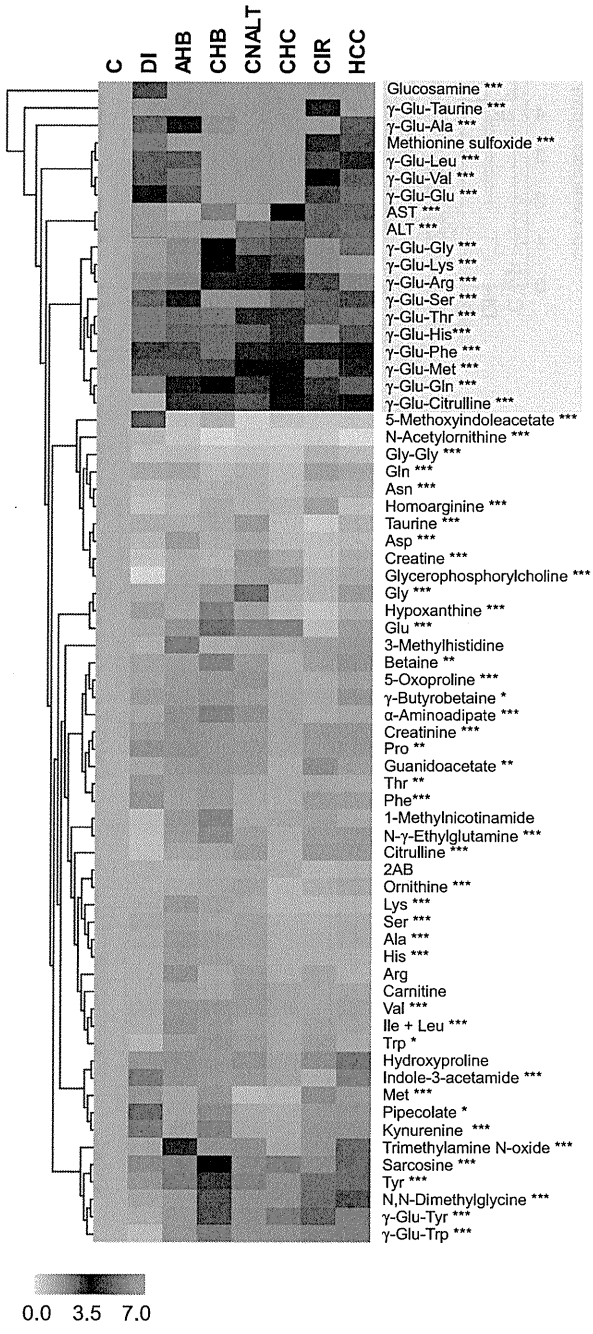

Fig. 1. Heat map representing the hierarchical clustering of 67 compounds in serum samples from controls and patients with various types of liver disease in both cohorts. Each row shows data for a specific metabolite or transaminase, and each column shows data for the healthy controls and patients with liver diseases. The compound concentration in each individual was divided by the average concentration in the healthy controls and the obtained values were then averaged again for each disease. The metabolites highlighted in blue showed large fold changes (disease/control ratios of >2.5) in an average of seven liver diseases. $^{*}p$ <0.05, $^{**}p$ <0.01, $^{***}p$ <0.0001, significance difference by the Kruskal–Wallis test. The compounds were clustered based on elucidation distances. Red and green denote relatively high and low concentrations, respectively, compared with the average concentration.

weights with those of the standards. Significant differences were observed among controls and liver diseases (p <0.0001; Kruskal–Wallis test) except for γ-Glu-Met in the validation data (Supplementary Tables 1 and 2). Correlational cluster analyses of 67 compounds showed that all the γ-glutamyl dipeptides except for γ-Glu-Tyr and γ-Glu-Trp were clustered with AST, ALT, and metabolites involved in oxidative stress responses, namely glucosamine [16] and methionine sulfoxide [17–19] (Fig. 1).

Statistical analysis and validation for biomarker discovery

From the serum samples obtained at YUH, we selected 89 liver disease patients including DI, AHB, CHB, CNALT, CHC, CIR, and HCC patients, and 53 healthy controls with no significant differences in the age distribution between the training and validation cohorts (Table 1). As shown in the whisker box plots for the training cohort (Fig. 2), the levels of γ-glutamyl dipeptides and of AST and ALT, as commonly used hepatocyte biomarkers, were increased in different patterns in comparison with C. For example, the AST and ALT levels were significantly increased in patients with DI, CHB, CHC, CIR, and HCC (p <0.05; Dunn's post-test), but not in those with AHB and CNALT (Fig. 2). On the other hand, significant increases were observed in the levels of γ-Glu-Ser, γ-Glu-Val, γ-Glu-Thr, γ-Glu-Leu, and γ-Glu-Phe (p <0.05; Dunn's post-test) in AHB and in the levels of all the γ-glutamyl derivatives of amino acids (p <0.05; Dunn's post-test) except for ophthalmate, γ-Glu-Thr, and γ-Glu-Trp in CNALT (Fig. 2 and Supplementary Table 1). Oxidative metabolites, methionine sulfoxide, and glucosamine were significantly increased in all diseases (p <0.05; Dunn's post-test) and in CHB, CNALT, and CHC (p <0.0001; Dunn's post-test), respectively (Fig. 2).

To assess their abilities to discriminate specific liver diseases from other liver diseases, we developed MLR models using combinations of several components of the γ-glutamyl dipeptides, transaminases, and oxidative metabolites using the training dataset. For example, an MLR model incorporating four selected biomarkers (γ-Glu-Ala, γ-Glu-Citrulline, γ-Glu-Thr, and γ-Glu-Phe) was able to differentiate HCC from the other groups (C, DI, AHB, CHB, CNALT, CHC, and CIR) with an area under the receiver-operating characteristic (ROC) curve (AUC) value of 0.762 (95% CI 0.647–0.877, $p = 0.00025$). The probability (p) of HCC is calculated by: $\log(p/(1-p)) = -1.87 - 1.13 \times$ γ-Glu-Ala $+ 3.51 \times$ γ-Glu-Citrulline $- 1.65 \times$ γ-Glu-Thr $+ 6.99 \times$ γ-Glu-Phe (Table 2). When the concentrations of γ-Glu-Ala, γ-Glu-Citrulline, γ-Glu-Thr, and γ-Glu-Phe are 1.7, 0.84, 0.54, and 0.34 μM, respectively, the probability of HCC is 65.5%. All the MLR models achieved high AUC values at statistically significant levels (between 0.754 and 0.972, p <0.011) (Fig. 3, Table 2 and Supplementary Table 3).

The developed MLR models were evaluated in a blinded manner using an independent cohort (YUH) consisting of 75 individuals who were not members of the training cohort (Supplementary Table 2). We found that all of the MLR models also produced high AUC values at statistically significant levels (between 0.707 and 0.993, p <0.023) (Fig. 3, Table 2 and Supplementary Table 3). Although C, CHB, and CHC were each differentiated from the other groups by a single γ-glutamyl dipeptide (γ-Glu-Phe, γ-Glu-Thr, and γ-Glu-Lys, respectively), the MLR models for the other diseases required multiple biomarkers to achieve accurate discrimination (Table 2). The odds ratios of ALT, AST, and methionine sulfoxide were close to 1.0 compared with the odds ratios of the γ-glutamyl dipeptides, indicating their

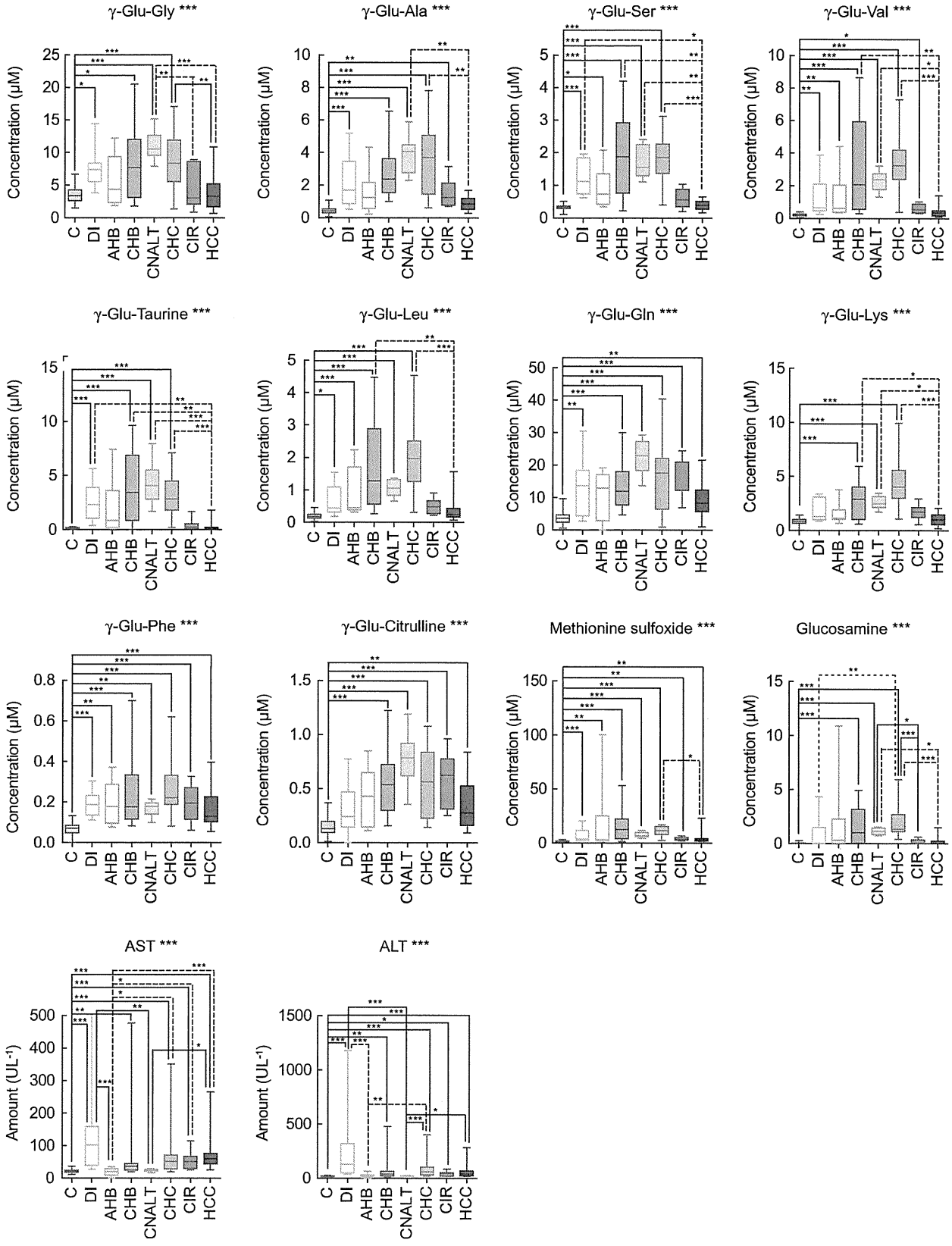
γ-Glu-Gly ***
γ-Glu-Ala ***
γ-Glu-Ser ***
γ-Glu-Val ***
γ-Glu-Taurine ***
γ-Glu-Leu ***
γ-Glu-Gln ***
γ-Glu-Lys ***
γ-Glu-Phe ***
γ-Glu-Citrulline ***
Methionine sulfoxide ***
Glucosamine ***
AST ***
ALT ***
Concentration (μM)
Amount (UL-1)
C
DI
AHB
CHB
CNALT
CHC
CIR
HCC

Table 2. Biomarkers for discriminating each liver disease selected by MLR models.

Group	Biomarker	Coefficient	95% CI		Odds ratio	95% CI		*p* value
C	(Intercept)	5.77	3.84	8.32	—	—	—	<0.0001
	γ-Glu-Phe	-58.2	-84.3	-39.0	5.16×10^{-26}	2.47×10^{-37}	1.15×10^{-17}	<0.0001
DI	(Intercept)	-3.08	-4.49	-1.94	—	—	—	<0.0001
	ALT	0.020	7.89×10^{-3}	0.034	1.02	1.01	1.03	2.00×10^{-3}
	γ-Glu-Citrulline	-1.55	-5.01	1.13	0.21	6.68×10^{-3}	3.11	0.31
AHB	(Intercept)	-1.52	-3.35	0.63	—	—	—	0.12
	AST	-0.057	-0.15	-4.96×10^{-3}	0.94	0.86	1.00	0.12
	Methionine sulfoxide	0.072	0.018	0.15	1.08	1.02	1.17	0.047
CHB	(Intercept)	-4.52	-6.33	-3.24	—	—	—	<0.0001
	γ-Glu-Thr	1.52	0.65	2.63	4.58	1.91	13.9	2.30×10^{-3}
CNALT	(Intercept)	-0.76	-3.15	1.94	—	—	—	0.55
	ALT	-0.16	-0.34	-0.049	0.85	0.71	0.95	0.032
	γ-Glu-Taurine	0.80	0.43	1.31	2.23	1.54	3.72	3.00×10^{-4}
CHC	(Intercept)	-4.73	-6.39	-3.47	—	—	—	<0.0001
	γ-Glu-Lys	1.27	0.85	1.82	3.57	2.34	6.14	<0.0001
CIR	(Intercept)	-2.79	-4.05	-1.55	—	—	—	<0.0001
	γ-Glu-Ala	1.80	0.42	3.52	6.05	1.52	33.7	0.020
	γ-Glu-Leu	-0.066	-3.06	2.24	0.94	0.047	9.42	0.96
	γ-Glu-Ser	-1.35	-5.35	1.86	0.26	4.77×10^{-3}	6.44	0.41
	γ-Glu-Taurine	-2.28	-5.07	-0.33	0.10	6.27×10^{-3}	0.72	0.064
HCC	(Intercept)	-1.87	-2.90	-0.90	—	—	—	2.00×10^{-4}
	γ-Glu-Ala	-1.13	-2.44	-0.14	0.32	0.087	0.87	0.050
	γ-Glu-Citrulline	3.51	0.45	7.00	33.4	1.57	1.10×10^{3}	0.033
	γ-Glu-Thr	-1.65	-5.12	0.49	0.19	5.95×10^{-3}	1.63	0.27
	γ-Glu-Phe	6.99	-0.52	14.7	1.09×10^{3}	5.92×10^{-1}	2.50×10^{6}	0.063

Note: The en-dashes in the 95% CI columns indicate that these values could not be calculated. Biomarker and coefficients are used in MLR model to calculate the probability of each disease. Intercept indicates the constant term in MLR models.

relatively lower contributions to the separation ability of the MLR models (Table 2). Overall, for all types of liver diseases, the MLR models mostly based on γ-glutamyl dipeptides provided complementary results, even in the second (validation) cohort.

γ-Glutamyl dipeptides as biomarkers for HCC and NAFLD

To evaluate the diagnostic potential of γ-glutamyl dipeptides for HCC, we compared their diagnostic abilities with that of AFP, an established marker for HCC (Fig. 4). We found that the MLR models using four γ-glutamyl dipeptides (γ-Glu-Ala, γ-Glu-Citrulline, γ-Glu-Thr, γ-Glu-Phe) (Table 2) were better at distinguishing HCC from CHC and CIR (AUC = 0.881) than AFP (AUC = 0.760) (Fig. 4).

We further investigated the biomarker specificities by comparing the serum γ-glutamyl dipeptide levels in GC and HCC patients (Supplementary Fig. 2 and Table 4). The analyses revealed significant differences, with the exception of γ-Glu-Phe, and the levels of γ-glutamyl dipeptides were notably low in GC.

Differences in the levels of γ-glutamyl dipeptides were also observed in NAFLD. The levels of six γ-glutamyl dipeptides (γ-Glu-Val, γ-Glu-Thr, γ-Glu-Leu, γ-Glu-His, γ-Glu-Phe, and γ-Glu-Arg) were significantly higher ($p < 0.05$; Mann–Whitney test) in SS than in NASH (Supplementary Fig. 3 and Table 5). Although further investigations are necessary, these dipeptides can be used as noninvasive biomarkers in rapid screening for SS and NASH.

Mechanism of γ-glutamyl dipeptide biosynthesis

To confirm the γ-glutamyl dipeptide biosynthesis pathway, the hepatic metabolism was investigated using a mouse model. In

Fig. 2. Representative whisker box plots of the serum levels of detected transaminases and metabolites in the training cohort. The horizontal lines indicate the upper median, median, and lower median, and the whiskers show the maximum and minimum levels. One plot for AST was outside the range (>500 U/L). *$p < 0.05$, **$p < 0.01$, ***$p < 0.0001$, significance difference by the Kruskal–Wallis test and Dunn's post-test for each marker and two groups in each marker, respectively.

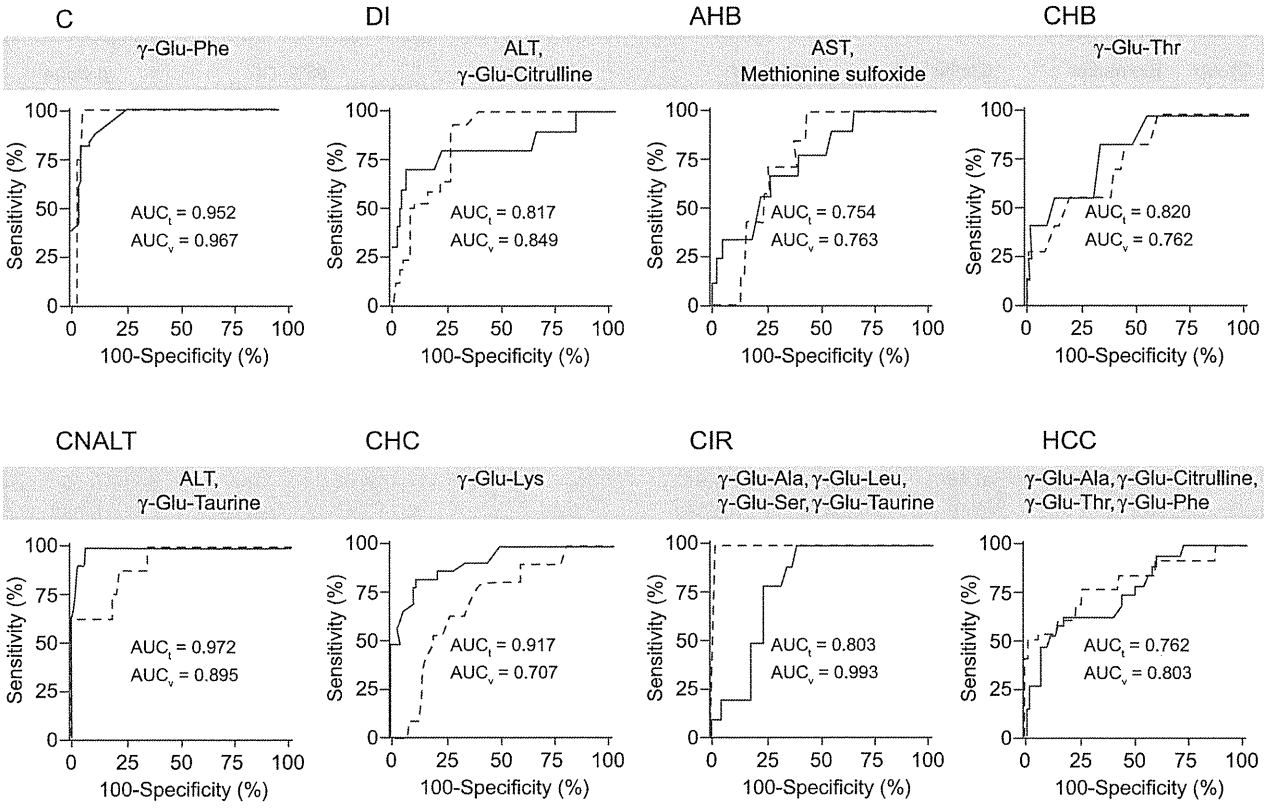

Fig. 3. ROC curve analyses of the ability of γ-glutamyl peptides alone or in combination with AST, ALT and methionine sulfoxide to discriminate each group from all other liver diseases and healthy controls. The solid and dashed curves represent the ROC curves for the training and validation cohorts, respectively. AUCt and AUCv in each panel indicate the AUC values in the training and validation cohorts, respectively. The group label indicates the discriminated group from all the other groups by an MLR model. The biomarkers in each panel were used in the MLR model for discriminating the group, e.g., ALT and γ-Glu-Taurine were the biomarkers for discriminating CNALT from the other groups. The coefficients and constant term of the MLR model of these biomarkers were summarized in Table 2.

acetaminophen (APAP)-treated mice [12], ophthalmate, a γ-glutamyl tripeptide, was synthesized through consecutive reactions with GCS and glutathione synthetase (GS), the same enzymes that play a role in GSH synthesis [12] (Fig. 5). Therefore, we investigated the alterations in the levels of hepatic amino acids, amines, γ-glutamyl dipeptides, and tripeptides after administration of buthionine sulfoximine (BSO), diethylmaleate (DEM) or APAP (Supplementary Fig. 4). BSO treatment resulted in GCS inhibition [20] and marked reductions in most of the hepatic γ-glutamyl dipeptide and tripeptide levels (Fig. 5 and Supplementary Fig. 4A). In contrast, DEM treatment led to GSH depletion by oxidation of the thiol group in GSH [21], resulting in GCS activation and considerable increases in the hepatic γ-glutamyl dipeptide and tripeptide levels compared with the controls (Fig. 5 and Supplementary Fig. 4A). The hepatic levels of several γ-glutamyl dipeptides and tripeptides were increased with concurrent GSH depletion in APAP-treated mice (Supplementary Fig. 4B and C). These results indicated that in mice, γ-glutamyl dipeptides and tripeptides were certainly synthesized via the ligation of glutamate by various amino acids through consecutive reactions with GCS and GS when GSH was depleted (Fig. 5). The identification details for the γ-glutamyl dipeptide biosynthetic pathway are described in the Supplementary data.

Discussion

Our analyses of 237 serum samples from patients with liver diseases and healthy controls revealed that γ-glutamyl dipeptides were increased in liver injuries and could provide specific information for different liver diseases. In APAP-induced liver injury in mice, ophthalmate, a γ-glutamyl tripeptide, was markedly increased as a byproduct of GSH synthesis [21] (Fig. 5 and Supplementary Fig. 4B). However, in liver diseases in humans, many γ-glutamyl dipeptides were primarily synthesized and secreted from hepatocytes into the blood (Figs. 1 and 5). Although the reason for the difference is unclear, it may be attributable to species differences in the levels and activities of enzymes and transporters [22,23].

In all types of liver disease, oxidative stress resulting from an imbalance between the production of reactive oxygen species (ROS) and the ability of a biological system to detoxify reactive intermediates plays a crucial role in the induction and progression of liver damage independently of its etiology [1]. In patients with hepatitis, oxidative stress is produced by inflammation induced by immunological mechanisms. Upon viral infection, NADPH oxidase produces ROS in neutrophils and macrophages, and ROS are also generated from free iron through the Fenton reaction [24–26]. ROS are further produced in hepatocytes upon

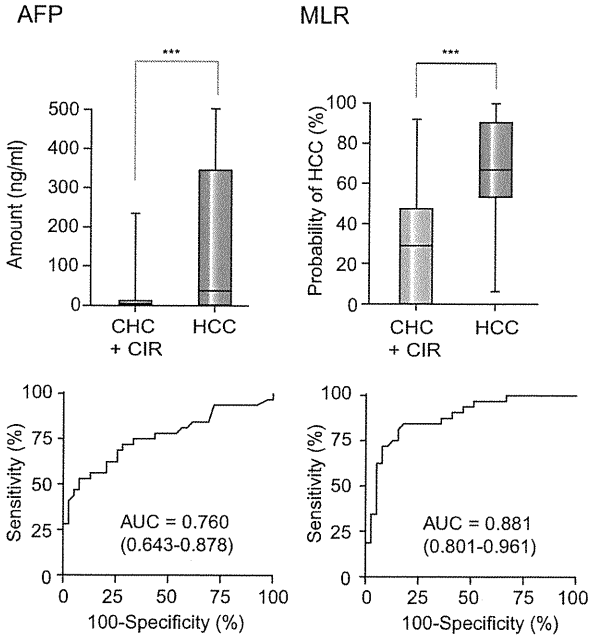

Fig. 4. Whisker box plots and ROC curves of AFP and MLR analyses based on γ-Glu-Ala, γ-Glu-Citrulline, γ-Glu-Thr and γ-Glu-Phe for discriminating patients with HCC ($n = 32$) from patients with CHC ($n = 35$) and CIR ($n = 18$).

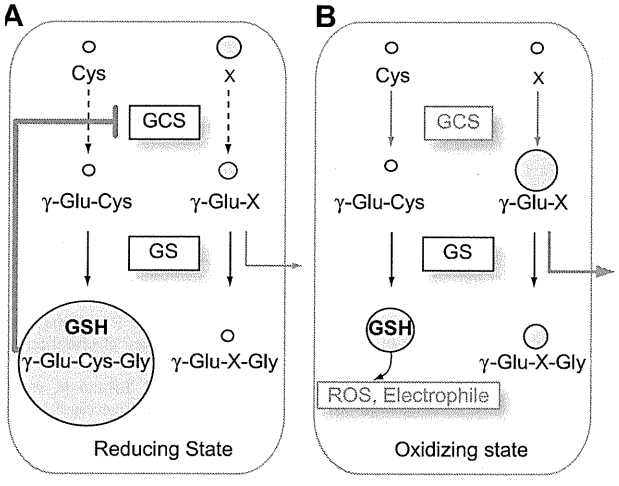

Fig. 5. Biosynthetic mechanism of γ-glutamyl peptides in hepatocytes under (A) reducing conditions and (B) oxidative stress. GCS is feedback-inhibited by GSH under reducing conditions and small amounts of γ-glutamyl dipeptides are synthesized. During oxidative stress, GSH is consumed, leading to GCS activation. This could result in biosynthesis of γ-glutamyl dipeptides, which are then effluxed across the hepatocellular membrane. γ-Glutamyl dipeptides and tripeptides are indicated by γ-Glu-X and Glu-X-Gly, respectively (X = amino acid or amine).

the release of inflammatory cytokines, such as tumor necrosis factor-α and interleukin-1β from inflammatory cells [27]. GSH is the most abundant antioxidant in hepatocytes, and helps to protect cells against ROS. Upon depletion of GSH, ROS induce oxidative stress resulting in liver damage, and reduced GSH levels have been demonstrated in various liver diseases [28–30].

Since γ-glutamyl dipeptides are byproducts of GSH synthesis catalyzed by GCS, their levels are indirect evidence for GSH production (Fig. 5). Different levels of γ-glutamyl dipeptides were observed in different types of liver disease and each γ-glutamyl dipeptide showed a somewhat different variation pattern among liver diseases (Fig. 2). This might be attributed to differences in hepatic levels of amino acids (the substrate of GCS) among liver diseases, though further studies are necessary to understand the details of this observation.

In healthy controls, the γ-glutamyl dipeptide levels were low. This occurred because under reducing conditions, the level of hepatic GSH was high and a small amount of GSH was biosynthesized (Fig. 5A). However, in the patients with liver diseases, GSH was consumed to neutralize the generated ROS, which in turn led to GCS activation, resulting in the biosynthesis of GSH together with γ-glutamyl dipeptides (Fig. 5B). Therefore, increased levels of γ-glutamyl dipeptides were observed in most liver injuries. Surprisingly, unlike AST and ALT, the levels of most γ-glutamyl dipeptides were markedly increased in asymptomatic individuals with AHB and CNALT (Fig. 2 and Supplementary Fig. 1), possibly because viral infection induced ROS generation followed by GSH depletion, which led to the biosynthesis of GSH and γ-glutamyl dipeptides (Fig. 5). We hypothesize that sufficiently high levels of GSH production neutralized ROS, resulting in lower incidences of AHB and CNALT.

There are relationships between liver diseases attributable to HCV infection and oxidative stress parameters, such as ROS, antioxidants, and inflammation. Oxidative stress increased with hepatic disease progression in HCV-infected patients [31]. Consistent with that report, among all the patients with HCV-related liver diseases, the serum levels of γ-glutamyl dipeptides, as indicators of hepatic GSH production, were markedly increased in CNALT and tended to decrease with disease progression (CNALT ⩾ CHC > CIR > HCC) (Fig. 2). These observations led us to conclude that at the time of viral infection (CNALT), a sufficient amount of GSH production can neutralize ROS and thus weaken the pathogenesis of liver damage. However, when GSH production falls below ROS generation, oxidative stress followed by inflammation is induced, resulting in the development and progression of liver diseases. Similarly, the levels of several γ-glutamyl dipeptides were significantly lower in NASH patients than in SS patients (Supplementary Fig. 3), indicating low levels of GSH production in NASH patients. Based on the present observations, we suggest that NASH is susceptible to oxidative stress and progression to liver fibrosis and cirrhosis.

HCC is one of the most common cancers in humans, and primarily develops in patients with chronic liver disease. Its early detection is important because effective treatments are available for the management of non-advanced cancers [32]. Until now, the diagnosis of HCC has relied on combinations of imaging techniques and measurements of the serum levels of AFP [33] and PIVKA-II [34]. Although they are reliable tumor markers for the diagnosis and monitoring of primary HCC, high levels of serum AFP and plasma PIVKA-II have also been observed in some gastric carcinomas [34,35]. However, the serum γ-glutamyl dipeptide levels in GC and HCC patients revealed significant differences, and the levels of several γ-glutamyl dipeptides was notably low in GC (Supplementary Fig. 2). We suspect that this occurred through differences in the tissue activities of the glutathione

system, since GSH is mainly synthesized *de novo* in the liver, and hypothesize that the γ-glutamyl dipeptide levels may reflect hepatic dysfunction.

Drug-induced hepatotoxicity is a frequent cause of liver injury, and the predominant clinical presentation is acute hepatitis and/or cholestasis. Overdoses of APAP, the most commonly used analgesic and antipyretic, can lead to possibly fatal hepatitis and several hundred deaths attributable to this drug occur annually in the United States. Our DI samples were from patients with so-called idiosyncratic hepatotoxicity, and the underlying mechanisms of this disease remain unclear. Interestingly, the changes in the serum levels of γ-glutamyl dipeptides were similar among the DI samples although the causative drugs differed widely and the mechanisms responsible for the development of hepatotoxicity may also be different. Our findings revealed that the amount of γ-glutamyl dipeptide production attributable to a reduction in the hepatocellular GSH concentration was a common feature in drug-induced idiosyncratic hepatotoxicity. With AUC values of 0.817 (training data) and 0.849 (validation data) (Supplementary Table 3), the serum levels of ALT and γ-Glu-Citrulline could be used to distinguish between DI patients on the one hand and patients with viral hepatitis infection and healthy controls on the other (Table 2). Therefore, we suggest that these compounds represent noninvasive biomarkers that facilitate rapid screening for DI.

In summary, our CE–TOFMS and LC–MS/MS metabolomics-based analyses of serum samples from patients with liver diseases showed quantitative differences in γ-glutamyl dipeptides in various liver diseases. Our highly specific set of γ-glutamyl dipeptides, transaminases, and methionine sulfoxide enabled us to discriminate among liver diseases including DI, AHB, CHB, CNALT, CHC, CIR, and HCC, indicating that they can be used as multiple biomarkers in rapid screening for different types and stages of liver disease. Furthermore, we have shown that γ-glutamyl dipeptide synthesis was catalyzed by GCS, the enzyme that is feedback-inhibited by GSH, and thus the levels of these biomarkers were indicative of hepatic GSH production. As observed in patients with HCV-related liver diseases and NAFLD, the serum γ-glutamyl dipeptide levels tended to decrease during the course of liver disease progression, indicating an increase in oxidative stress resulting from decreased GSH production during liver disease progression. Therefore, γ-glutamyl dipeptide measurement can potentially provide valuable information about the hepatic reduction–oxidation state to gain insights into the role of oxidative stress in the pathogenesis and progression of liver diseases.

Conflict of interest

The Authors who have taken part in this study declared that they do not have anything to disclose regarding funding or conflict of interest with respect to this manuscript.

Financial support

This work was supported by Health and Labour Sciences Research Grants "Research on Biological Markers for New Drug Development" (T.S.) and "Research on Risk of Chemical Substances" (T.S.). Additional support was obtained through grants from the Ministry of Education, Culture, Sports, Science and Technology (MEXT) for a Global COE Program entitled "Human Metabolomic Systems Biology" in Life Sciences (T.S., M.T. and M.S.) and the ERATO Gas Biology Project (M.S.), as well as research funds from the Yamagata Prefectural Government and City of Tsuruoka.

Supplementary data

Supplementary data associated with this article can be found, in the online version, at doi:10.1016/j.jhep.2011.01.031.

References

[1] Loguercio C, Federico A. Oxidative stress in viral and alcoholic hepatitis. Free Radic Biol Med 2003;34:1–10.
[2] Brunt EM. Nonalcoholic steatohepatitis. Semin Liver Dis 2004;24:3–20.
[3] Younossi ZM, Jarrar M, Nugent C, Randhawa M, Afendy M, Stepanova M, et al. A novel diagnostic biomarker panel for obesity-related nonalcoholic steatohepatitis (NASH). Obes Surg 2008;18:1430–1437.
[4] Piccinino F, Sagnelli E, Pasquale G, Giusti G. Complications following percutaneous liver biopsy. A multicentre retrospective study on 68,276 biopsies. J Hepatol 1986;2:165–173.
[5] Bolukbas C, Bolukbas FF, Horoz M, Aslan M, Celik H, Erel O. Increased oxidative stress associated with the severity of the liver disease in various forms of hepatitis B virus infection. BMC Infect Dis 2005;5:95.
[6] Sreekumar A, Poisson LM, Rajendiran TM, Khan AP, Cao Q, Yu J, et al. Metabolomic profiles delineate potential role for sarcosine in prostate cancer progression. Nature 2009;457:910–914.
[7] Bogdanov M, Matson WR, Wang L, Matson T, Saunders-Pullman R, Bressman SS, et al. Metabolomic profiling to develop blood biomarkers for Parkinson's disease. Brain 2008;131:389–396.
[8] Wang C, Kong H, Guan Y, Yang J, Gu J, Yang S, et al. Plasma phospholipid metabolic profiling and biomarkers of type 2 diabetes mellitus based on high-performance liquid chromatography/electrospray mass spectrometry and multivariate statistical analysis. Anal Chem 2005;77:4108–4116.
[9] Sabatine MS, Liu E, Morrow DA, Heller E, McCarroll R, Wiegand R, et al. Metabolomic identification of novel biomarkers of myocardial ischemia. Circulation 2005;112:3868–3875.
[10] Kenny LC, Dunn WB, Ellis DI, Myers J, Baker PN, Consortium TG, et al. Novel biomarkers for pre-eclampsia detected using metabolomics and machine learning. Metabolomics 2005;1:227–234.
[11] Soga T, Ohashi Y, Ueno Y, Naraoka H, Tomita M, Nishioka T. Quantitative metabolome analysis using capillary electrophoresis mass spectrometry. J Proteome Res 2003;2:488–494.
[12] Soga T, Baran R, Suematsu M, Ueno Y, Ikeda S, Sakurakawa T, et al. Differential metabolomics reveals ophthalmic acid as an oxidative stress biomarker indicating hepatic glutathione consumption. J Biol Chem 2006;281:16768–16776.
[13] Soga T, Igarashi K, Ito C, Mizobuchi K, Zimmermann HP, Tomita M. Metabolomic profiling of anionic metabolites by capillary electrophoresis mass spectrometry. Anal Chem 2009;81:6165–6174.
[14] Shintani T, Iwabuchi T, Soga T, Kato Y, Yamamoto T, Takano N, et al. Cystathionine beta-synthase as a carbon monoxide-sensitive regulator of bile excretion. Hepatology 2009;49:141–150.
[15] Goto S, Okuno Y, Hattori M, Nishioka T, Kanehisa M. LIGAND: database of chemical compounds and reactions in biological pathways. Nucleic Acids Res 2002;30:402–404.
[16] Kaneto H, Xu G, Song KH, Suzuma K, Bonner-Weir S, Sharma A, et al. Activation of the hexosamine pathway leads to deterioration of pancreatic beta-cell function through the induction of oxidative stress. J Biol Chem 2001;276:31099–31104.
[17] Levine RL, Berlett BS, Moskovitz J, Mosoni L, Stadtman ER. Methionine residues may protect proteins from critical oxidative damage. Mech Ageing Dev 1999;107:323–332.
[18] Babior BM. Phagocytes and oxidative stress. Am J Med 2000;109:33–44.
[19] Vogt W. Oxidation of methionyl residues in proteins: tools, targets, and reversal. Free Radic Biol Med 1995;18:93–105.
[20] Griffith OW, Meister A. Potent and specific inhibition of glutathione synthesis by buthionine sulfoximine (*S-n*-butyl homocysteine sulfoximine). J Biol Chem 1979;254:7558–7560.
[21] Zalups RK, Lash LH. Depletion of glutathione in the kidney and the renal disposition of administered inorganic mercury. Drug Metab Dispos 1997;25:516–523.

[22] Ishizuka H, Konno K, Shiina T, Naganuma H, Nishimura K, Ito K, et al. Species differences in the transport activity for organic anions across the bile canalicular membrane. J Pharmacol Exp Ther 1999;290:1324–1330.
[23] Mainwaring GW, Williams SM, Foster JR, Tugwood J, Green T. The distribution of theta-class glutathione *S*-transferases in the liver and lung of mouse, rat and human. Biochem J 1996;318:297–303.
[24] Marrogi AJ, Khan MA, van Gijssel HE, Welsh JA, Rahim H, Demetris AJ, et al. Oxidative stress and p53 mutations in the carcinogenesis of iron overload-associated hepatocellular carcinoma. J Natl Cancer Inst 2001;93:1652–1655.
[25] Toyokuni S, Okamoto K, Yodoi J, Hiai H. Persistent oxidative stress in cancer. FEBS Lett 1995;358:1–3.
[26] Sutton A, Nahon P, Pessayre D, Rufat P, Poire A, Ziol M, et al. Genetic polymorphisms in antioxidant enzymes modulate hepatic iron accumulation and hepatocellular carcinoma development in patients with alcohol-induced cirrhosis. Cancer Res 2006;66:2844–2852.
[27] Koike K, Miyoshi H. Oxidative stress and hepatitis C viral infection. Hepatol Res 2006;34:65–73.
[28] Boya P, de la Pena A, Beloqui O, Larrea E, Conchillo M, Castelruiz Y, et al. Antioxidant status and glutathione metabolism in peripheral blood mononuclear cells from patients with chronic hepatitis C. J Hepatol 1999;31:808–814.
[29] Tanyalcin T, Taskiran D, Topalak O, Batur Y, Kutay F. The effects of chronic hepatitis C and B virus infections on liver reduced and oxidized glutathione concentrations. Hepatol Res 2000;18:104–109.
[30] Moriya K, Nakagawa K, Santa T, Shintani Y, Fujie H, Miyoshi H, et al. Oxidative stress in the absence of inflammation in a mouse model for hepatitis C virus-associated hepatocarcinogenesis. Cancer Res 2001;61:4365–4370.
[31] Sumida Y, Nakashima T, Yoh T, Nakajima Y, Ishikawa H, Mitsuyoshi H, et al. Serum thioredoxin levels as an indicator of oxidative stress in patients with hepatitis C virus infection. J Hepatol 2000;33:616–622.
[32] Bruix J. Treatment of hepatocellular carcinoma. Hepatology 1997;25:259–262.
[33] Szklaruk J, Silverman PM, Charnsangavej C. Imaging in the diagnosis, staging, treatment, and surveillance of hepatocellular carcinoma. Am J Roentgenol 2003;180:441–454.
[34] Kudo M, Takamine Y, Nakamura K, Shirane H, Uchida H, Kasakura S, et al. Des-gamma-carboxy prothrombin (PIVKA-II) and alpha-fetoprotein-producing IIc-type early gastric cancer. Am J Gastroenterol 1992;87:1859–1862.
[35] Takano S, Honda I, Watanabe S, Soda H, Nagata M, Hoshino I, et al. PIVKA-II-producing advanced gastric cancer. Int J Clin Oncol 2004;9:330–333.

STEM CELLS AND DEVELOPMENT
Volume 20, Number 9, 2011

DOI: 10.1089/scd.2011.0074

Potential Therapeutic Application of Intravenous Autologous Bone Marrow Infusion in Patients with Alcoholic Liver Cirrhosis

Takafumi Saito,[1] Kazuo Okumoto,[1] Hiroaki Haga,[1] Yuko Nishise,[1] Rika Ishii,[1] Chikako Sato,[1] Hisayoshi Watanabe,[1] Akio Okada,[2] Motoki Ikeda,[2] Hitoshi Togashi,[3] Tsuyoshi Ishikawa,[4] Shuji Terai,[4] Isao Sakaida,[4] and Sumio Kawata[1]

The present study was conducted to evaluate the application and efficacy of autologous bone marrow infusion (ABMi) for improvement of liver function in patients with alcoholic liver cirrhosis (ALC). Five subjects and 5 control patients with ALC who had abstained from alcohol intake for 24 weeks before the study were enrolled. Autologous bone marrow cells were washed and injected intravenously, and the changes in serum liver function parameters, and the level of the type IV collagen 7S domain as a marker of fibrosis, were monitored for 24 weeks. The distribution of activated bone marrow was assessed by indium-111-chloride bone marrow scintigraphy. The number of cells infused was $8.0 \pm 7.3 \times 10^9$ (mean ± standard error). The serum levels of albumin and total protein and the prothrombin time were significantly higher during the follow-up period after ABMi than during the observation period in treated patients, whereas no such changes were observed in the controls. In the patients who received ABMi, the Child-Pugh score decreased in all 3 who were classified as class B; the serum levels of type IV collagen 7S domain improved in 4 of the 5 patients; and bone marrow scintigraphy demonstrated an increase of indium-111-chloride uptake in 3 of the 4 patients tested. ABMi for patients with ALC helps improve liver function parameters in comparison with observation during abstinence and ameliorates the degree of fibrosis in terms of serum markers and bone marrow activation in most cases.

Introduction

Liver cirrhosis is the end stage of chronic liver disease, and it is associated with many serious systemic complications resulting from both liver failure and portal hypertension. This condition has a poor prognosis and is difficult to treat. Liver transplantation is the only curative remedy, but it is associated with many problems such as donor shortage, surgical complications, rejection, and high cost. As an alternative approach, regenerative cell therapy using stem cells is now being investigated. In particular, multipotent stem cells present in bone marrow (BM) are a promising candidate for this purpose, and clinical trials aiming at therapy of cardiovascular diseases have been performed [1,2].

BM cells have been shown to be capable of differentiating into the liver cell lineage, and transplantation of BM cells has considerable potential for regeneration of liver tissue [3–6]. The degree of liver function and fibrosis as well as survival rate have been shown to improve significantly as a result of BM cell transplantation in animal models of severe liver injury [7,8]. We have experimentally investigated the potential of BM stem cells to differentiate into the hepatocyte lineage both in vitro or in vivo with a view to possible application for clinical trials aimed at liver regeneration [9–12]. In this context, the effectiveness of CD34+ hematopoietic stem cell injection into the liver via the portal vein or hepatic artery had been shown to improve the serum levels of albumin and bilirubin [13,14]. Our research group has already reported the therapeutic effectiveness of whole-BM peripheral infusion, referred to as autologous BM cell infusion (ABMi) therapy for patients with cirrhosis with hepatitis B or C [15,16].

Alcoholic liver injury is a common liver disease worldwide. Although disease activity may be decreased by abstinence in the initial phase, it eventually progresses to cirrhosis and finally to death unless patients receive appropriate therapeutic intervention for both liver injury and alcohol abuse. Even if patients discontinue alcohol intake, those in whom the disease has progressed to advanced cirrhosis with marked liver fibrosis have a poor prognosis because of

Departments of [1]Gastroenterology and [2]Radiology, Yamagata University School of Medicine, Yamagata, Japan.
[3]Health Administrative Center, Yamagata University, Yamagata, Japan.
[4]Department of Gastroenterology and Hepatology, Yamaguchi University Graduate School of Medicine, Ube, Yamaguchi, Japan.

serious complications and liver cell dysfunction. Therefore, such patients require some form of liver-regenerative therapy, as well as abstinence, to improve the liver function. Since such patients are free of pathogens such as hepatitis B or hepatitis C that cause continuous liver necroinflammation, ABMi might facilitate a degree of liver regeneration if abstinence is maintained along with appropriate nutritional care. Pai et al. reported that autologous infusion of expanded mobilized BM-derived CD34+ cells into patients with alcoholic liver cirrhosis (ALC) via the hepatic artery improved the serum levels of both bilirubin and transaminase, as well as the Child-Pugh score [17].

To investigate the effectiveness of ABMi for patients with ALC, we applied it to such patients and examined the resulting changes in liver function parameters. In addition, using indium-111-chloride (^{111}In) BM scintigraphy, we tracked the infused BM cells after ABMi.

Patients and Methods

Patients

Patients with a diagnosis of advanced liver cirrhosis due to alcoholic liver injury were enrolled. All the patients were negative for both anti-hepatitis C virus antibody and hepatitis B surface antigen and had a history of excessive alcohol consumption exceeding 60 g/day of ethanol for >5 years. The patients were interviewed, and those who had abstained for >24 weeks before the interview were entered into the study. The inclusion criteria for clinical parameters were as follows: platelet count >50,000/mm^3, total bilirubin <3 mg/dL, and absence of liver cancer on computed tomography (CT). Both heart and lung function were screened to confirm whether general anesthesia was possible. As a control group, we used patients who were not given ABMi, but who agreed to the use of their clinical data for study. Those patients had also been diagnosed as having ALC, and were matched to the subjects who received ABMi for age, sex, medication, and various biochemical parameters; their liver function parameters were compared with those of the subjects who received ABMi during the study period.

Autologous BM cell preparation and infusion into patients

A total of 400 mL BM was harvested from the ilium according to the standard procedure under general anesthesia and collected in a plastic bag containing heparin. After fat had been removed from the top of the bag, hydroxyethyl starch was added to a final concentration of 1%. Red blood cells were precipitated after 40 min of incubation at room temperature. We used an automated bench-top device (Cytomate; Takara Bio Inc., Otsu, Shiga, Japan), which is a functionally closed system incorporating a spinning membrane connected to a filter wash bag, for washing and concentrating the mononuclear cells (MNCs). The final cell products were washed, concentrated, and made up to a final volume of 105 mL. Five milliliters of the final cell product was subjected to the trypan blue dye exclusion test, endotoxin test, and fluorescence-activated cell sorting analysis. CD34+, CD44+, CD45+, and CD117+ cells were determined by flow cytometry at the central laboratory of SRL Inc., Tokyo, Japan. At 6 h after BM harvest, the final MNCs preparation was administered to each patient via the cubital vein by drip infusion. All the study protocols were approved by the ethics committee of Yamagata University School of Medicine, and written informed consent was obtained from all participants.

Follow-up of serological tests for liver function and fibrosis

The patients were followed up, and laboratory data were analyzed for 48 weeks in total, which included analyses once a month for 24 weeks before and after ABMi therapy. Patients who consumed more than 20 g alcohol/day during the analysis period were considered to have dropped out and excluded from further analysis. Primary outcomes were the safety and feasibility of ABMi therapy for ALC. The serum parameters representing liver function, including serum albumin, total protein, and prothrombin time, were evaluated before and after ABMi therapy. The Child-Pugh score calculated by summing the total points for the serum levels of albumin and total bilirubin, prothrombin time, ascites, and encephalopathy was used to evaluate the overall condition of patients with cirrhosis. To evaluate the changes in the degree of liver fibrosis in patients receiving ABMi, the serum levels of the type IV collagen 7S domain was monitored during the follow-up period. The liver function parameters of the control patients who succeeded in maintaining abstinence were followed up for the same period as that of patients who received ABMi.

Liver function calculated by single photon emission CT analysis

Analysis of the liver using single photon emission CT (SPECT) with a radiolabeled, specific hepatic binding protein, technetium 99m galactosyl-human serum albumin (Tc-GSA), was carried out according to the procedure we have previously reported [18]. SPECT analysis is useful for assessment of hepatic functional reserve [19,20]. Briefly, Tc-GSA (185 MBq) was injected intravenously, and SPECT data were obtained from 12 min 30 s to 17 min 30 s after the injection using a triple-headed camera (MULTISPECT 3; Siemens Medical Systems, Erlangen, Germany). The liver uptake ratio, that is, the actual percentage of the administered Tc-GSA dose incorporated into the liver, was quantified by calculating the percentage of the hepatic SPECT value relative to the preinjection syringe value. The liver volume was obtained from the SPECT data and calculated by the outline extraction method to determine the functional liver volume in cm^3. The liver uptake ratio was then divided by the functional liver volume to obtain the liver uptake ratio per unit volume (liver uptake density; %/cm^3). We assessed the obtained liver uptake density values of patients receiving ABMi before the treatment and 2 weeks after.

BM imaging by ^{111}In scintigraphy

BM scintigraphy using ^{111}In was performed in 4 of the 5 patients before and 1 week after ABMi therapy. BM scintigraphy is useful for evaluating the distribution of activated BM, mainly hematopoietic stem cells. The scintigraphy was conducted 48 h after an intravenous injection of ^{111}In (74 MBq). The total ^{111}In count was divided by the total number of pixels on the computer screen to obtain the ^{111}In